A Cross-Layer Approach to Mixed-Control Topology Management for MANETs

Marco Carvalho, Adrian Granados, Sankrith Subramanian and Carlos Perez
Institute for Human and Machine Cognition
{mcarvalho, agranados, ssubramanian, cperez}@ihmc.us

***Abstract*—Topology Control (TC) algorithms are generally applied to tactical network environments to create or maintain connectivity graphs with specific topological properties. In the context of this work, network topology defines the connectivity and link properties between nodes in the network. While protocols in the communications stack are traditionally designed to adapt to different traffic demands and underlying changes in network topology, TC algorithms offer an opportunity for applications to become proactive, and to drive changes in network topology. In most cases, topology control is achieved through a number of independent control strategies such as power management, node mobility or spectrum allocation, each of which operates at a different time scale, with different constraints and capabilities. In this work we introduce a mixed topology control strategy for highly dynamic tactical networks. The proposed approach combines two controllers (one for transmit power and one for node mobility) to enable a self-regulating link maintenance algorithm that compensates for short term variations in link conditions while supporting a more permanent, slower adaptation based on node position. While applied for transmit power and node mobility in this paper, the approach is generic enough to be extended to different parameters. After describing the control formulation and its stability analysis, we introduce simple leader-follower scenarios simulated in NS-3 to illustrate the capabilities and properties of the proposed approach.**

I. Introduction

Mobile ad hoc networks (MANETs) are often characterized as dynamic wireless networks that do not rely on any form of fixed supporting infrastructure to operate. Conventionally, communication protocols and services in MANETs are designed to adapt in response to traffic demands and changes in network topology and link characteristics, which can occur, for instance, due to node mobility and physical layer settings (power, frequency, etc). In most cases, however, the changes in the underlaying network topology are only indirectly perceived. For example, the loss or degradation of a data link in an airborne network will lead to localized packet losses that will trigger changes in the routing tables, and eventually affect the behavior of transport protocols. Thus, the effects of changes in the underlying network topology to the communications stack are indirect, and often delayed.

The concept of topology control (TC) in wireless networks introduces the notion that applications or higher level protocols drive changes in the underlying radio frequency topology. These changes aim to enable network services and better support certain capabilities and quality of service requirements.

Most TC methods focus on the control of one metric, such as power management, frequency management or node mobility. Considered in isolation, each of these approaches provide a different level of control, working on different time scales. Power management, for instance, can be achieved in short time scales for topology control when compared with node mobility-based approaches. However, for practical deployments, there is a need for a comprehensive strategy capable to combine adaptation mechanisms at all levels, providing a smooth transition in topology even in highly dynamic environments.

In this paper we introduce a methodology for topology control that combines multiple control variables to enable faster and more efficient topology control algorithms for QoS maintenance. As a proof of concept of our proposed method, we combine two metrics that operate at different time scales (power control and mobility) to create a mixed control strategy for topology control. After describing an illustrative scenario of interest, we will introduce and analyze the proposed control strategy, concluding our work with the discussion and analysis of our experimental results.

II. Related Work

Topology control for ad hoc and sensor wireless networks is certainly not a new topic. Some of the earliest research in topology control for packet radios dates from the mid-80's [1] and primarily focused on power control. In the subsequent years numerous research efforts in the field continue to appear, primarily associated with attempts to reduce energy consumption [2] [3] and interference [4] [5] [6] in multi-hop wireless networks.

Alternative control approaches based on node mobility [7] [8] and spectrum management, or channel allocations [9] have been proposed. There are comprehensive surveys on topology control in the literature [10] [11], and more recently, even application driven topology control strategies [12].

In the majority of these examples, the different topology control algorithms focus on a single control variable such as power, mobility or channel allocation. In this work, our primary interest is not on distributed algorithms for multi-hop networks, but on the design of mixed input topology control algorithms. In particular, we will explore a joint control strategy that operates in different time-scales, enabling new capabilities for link stability. The link control strategy

978-1-4244-8180-4/10/$26.00 ©2010 IEEE

introduced here can be applied as part of centralized or distributed algorithms for wireless networks.

III. Problem Statement and Illustrative Scenario

Our scenario of interest illustrates an airborne network environment. We have considered a leader-follower scenario where two unmanned vehicles (Fig. 1) engage in a target tracking mission. While the leader vehicle directly engages to maintain close tracking of a target, the follower attempts to maintain a continuous support and relay connectivity.

Due to the differences in capabilities of each platform, the follower is responsible for maintaining a critical control link to the leader platforms. While remote operators are free to navigate the leaders, the follower node is responsible for maintaining the control channel within strict levels of service and reliability.

The connectivity link between the UAVs is affected by the distance between the platforms and the relative banking, so the main task of the follower platform is to ensure a minimum level of QoS requirement between the two platforms so the communication channel provided to the leader can be properly maintained at all times.

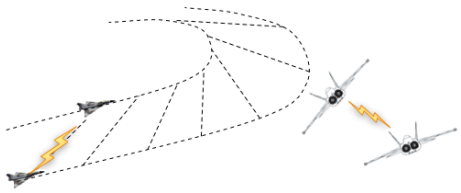

Fig. 1. Autonomous flight coordination for link state maintenance

Let us consider that, for all intents and purposes, the metric of interest for QoS support is SINR (Signal to Interference plus Noise Ratio). We could apply the same approach to other metrics, or combinations of metrics, but we will use a single SINR metric to simplify the discussions.

While engaged with the target, the leader node receives a continuous command stream through the follower, and periodically reports to the follower a short term average SINR of the control channel. The follower node, operating as a relay, closely monitors the quality of the control channel and continuously adjusts its relative distance from the leader to maintain the required level of service.

However, for a given constant transmit power level, it is likely that delays in response due to the dynamics of each platform will lead to significant variations on SINR. For example, when perceiving a variation of SINR due to a change in acceleration or banking of the leader, the follower must adjust its own position accordingly to maintain the desired levels of SINR.

Fig. 2 illustrates the results of the NS-3 simulation, where the first graph 2(a) describes SINR measured by the leader based on the transmissions received from the follower, and 2(b) shows the relative distance between the two platforms. When the leader platform initiates a maneuver, there is a

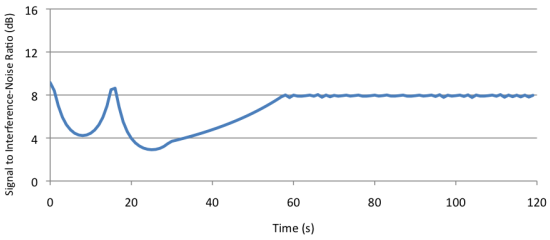

(a) SINR of the leader

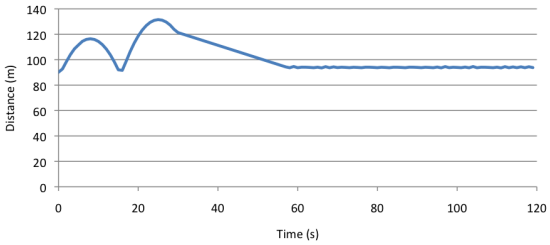

(b) Distance between follower and leader

Fig. 2. Mobility control without power control

variation (increase) in distance between nodes. Hence, packets arriving at the follower node are received with increasingly lower SINR, violating the QoS requirements of 8dB SINR. When the follower detects a violation, it immediately initiates the correction of the relative position to reach the desired SINR. However, the dynamics on the platforms create a period of adjustment (from 0 to 60 seconds) required for the follower to reposition itself in relation to the leader. During this adaptation period, the delay to adjust position causes a violation of the SINR requirements (4dB during some periods).

One way to avoid the delays induced by system dynamics would be to manipulate power, as opposed to relative position. In that case, upon detecting a QoS violation, the follower would increase its own transmit power to mitigate the problem. Despite the detection delay, the power management strategy would be faster, and would avoid the variations on SINR, but only until its maximum transmit level, when there would be a possible disconnection between the nodes.

Alternatively, a combined control strategy could leverage the best capabilities of each control variable, relying on power management to compensate for high frequency variations of SINR and mobility control to compensate for the long term trends in SINR variation. In the next section, we introduce a mixed control strategy that aims to provide a robust response for SINR maintenance, properly activating and mixing power and mobility as a function of the QoS requirements.

IV. Network Model

SINR is a widely used measure to quantify the quality of the radio link between 2 nodes. SINR, denoted by $x(\cdot) \in \mathbb{R}$, at instant $l \in \mathbb{Z}$ between the transmitter and the receiver is defined as

$$x(l) = 10\log\left(\frac{g(l)P(l)}{\eta(l)}\right), \tag{1}$$

where $\eta(\cdot) \in \mathbb{R}$ is the receiver noise, $P(l) \in \mathbb{R}$ is the transmit power, and $g(\cdot) \in \mathbb{R}$ is the channel gain [13] defined as

$$g(l) = g_{d_0}\left(\frac{d(l)}{d_0}\right)^{-\kappa} 10^{0.1\delta(l)}|X(l)|^2, \tag{2}$$

where $d(\cdot) \in \mathbb{R}$ is the distance between the nodes, $\delta(\cdot) \in \mathbb{R}$ is the log-normal shadowing, $\mathbb{R}$ is the power of the fading envelope, and g_{d_0} is the near-field gain given by [14]

$$g_{d_0} = \frac{G_t G_r \lambda^2}{(4\pi)^2 d_0^2 L}, \qquad d_f \le d_0 \le d(l), \tag{3}$$

where G_t is the transmitter antenna gain, G_r is the receiver antenna gain , λ is the wavelength in meters, L is the system-loss factor, d_0 is the distance between the transmitter and receiver antenna, and $d_f = 6m$ is the Fraunhofer distance. The antenna gains G_t and G_r and the loss factor L are assumed to be 1 without loss of generality. Taking the first difference of (1), we get

$$\begin{aligned}\frac{\Delta x(l)}{T_s} =& \frac{x(l+1)-x(l)}{T_s}\\ =& \frac{1}{T_s}\Big[10\log\left(\frac{g(l+1)}{g(l)}\right) + 10\log\left(\frac{P(l+1)}{P(l)}\right)\\ &+ 10\log\left(\frac{\eta(l+1)}{\eta(l)}\right)\Big],\end{aligned} \tag{4}$$

where T_s is the sampling time of the system.

Substituting (2) in (4), we get

$$\begin{aligned}x(l+1) - x(l) =& \\ & 10\log\left(\frac{(d(l+1))^{-\kappa}\, 10^{0.1\delta(l+1)}|X(l+1)|^2}{(d(l))^{-\kappa}\, 10^{0.1\delta(l)}|X(l)|^2}\right)\\ &+ 10\log\left(\frac{P(l+1)}{P(l)}\right) + 10\log\left(\frac{\eta(l+1)}{\eta(l)}\right)\\ &+ \xi(l)\end{aligned}$$

$$\begin{aligned}\Rightarrow x(l+1) =& 10\log\left(\frac{10^{0.1\delta(l+1)}|X(l+1)|^2}{10^{0.1\delta(l)}|X(l)|^2}\right)\\ &+ 10\log\left(\frac{\eta(l+1)}{\eta(l)}\right)\\ &- \kappa 10\log\left(\frac{d(l+1)}{d(l)}\right) + 10\log\left(\frac{P(l+1)}{P(l)}\right)\\ &+ x(l) + \xi(l)\\ \Rightarrow x(l+1) =& f_1(l) + u(l) + x(l) + \xi(l),\end{aligned}$$

where $f(l) \in \mathbb{R}$ is defined as

$$\begin{aligned}f(l) =& 10\log\left(\frac{10^{0.1\delta_i(l+1)}|X(l+1)|^2}{10^{0.1\delta(l)}|X(l)|^2}\right)\\ &+ 10\log\left(\frac{\eta(l+1)}{\eta(l)}\right),\end{aligned}$$

$$u(l) = 10\log\left(\frac{P(l+1)}{P(l)}\right) - \kappa 10\log\left(\frac{d(l+1)}{d(l)}\right) \tag{5}$$

is the controller, and $\xi(l)$ is the measurement noise.

V. Control Development

A. Control Objective

The QoS for the 2-node network can be quantified by the ability of the SINR to remain within a specified operating range with upper and lowers limits, $\gamma_{\min}, \gamma_{\max} \in \mathbb{R}$ defined as

$$\gamma_{\min} \le x_i(l) \le \gamma_{\max}. \tag{6}$$

Keeping the SINR above the minimum threshold eliminates signal dropout, whereas remaining below the upper threshold minimizes interference to adjacent nodes. The control objective is to regulate the SINR to a target value, denoted by $\gamma \in \mathbb{R}$, while ensuring that the SINR remains between the specified lower and upper limits. To quantify this objective, a regulation error is defined as $e(l) \in \mathbb{R}$ where

$$e(l) = x(l) - \gamma. \tag{7}$$

B. Closed-Loop Error System

Taking the first difference of (7),

$$\begin{aligned}\Delta e(l) =& \Delta x(l)\\ =& 10\log\left(\frac{10^{0.1\delta(l+1)}|X(l+1)|^2}{10^{0.1\delta(l)}|X(l)|^2}\right)\\ &+ 10\log\left(\frac{\eta(l+1)}{\eta(l)}\right) + u(l) + \xi(l).\end{aligned} \tag{8}$$

In practice $g(l)$ cannot take arbitrarily large values because the received power cannot exceed the transmitted power. Hence, fading power $|X_i(\cdot)|^2$ is bounded and non-zero, and

$$10\log\left\{\left|\frac{|X(l+1)|^2}{|X(l)|^2}\right|\right\} \le c_1. \tag{9}$$

Shadowing occurs due to the different clutter levels in the propagation path, and hence nodes at a different location but at the same distance from the transmitter might suffer different path losses.

The shadowing variable, $\delta(\cdot)$ is a zero-mean Gaussian distributed variable (in dB) [14]. Gaussian random process provides a good model for log-normal shadowing. However, there is a non-zero probability that $\delta(\cdot)$ might have a value of ∞. In practice, the shadowing process can be assumed to give finite values of $\delta(\cdot)$ since the path loss spread can be assumed to be finite about a distance-dependent mean. Hence, the norm $|\delta(l+1) - \delta(l)|$ can be upper bounded by some positive scalar as

$$|\delta(l+1) - \delta(l)| \le c_2, \tag{10}$$

the measurement noise is assumed to be bounded, and hence

$$|\xi(l, x)| \le c_3, \tag{11}$$

and the receiver thermal noise is assumed to be bounded and nonzero

$$10\log\left\{\left|\frac{\eta(l+1)}{\eta(l)}\right|\right\} \le c_5. \tag{12}$$

The controller is designed based on the subsequent stability analysis as

$$u(l) = -\left(k_1 + k_2\right) e(l), \tag{13}$$

Substituting (13) in (5), we get

$$\frac{P(l+1)}{(d(l+1))^{\kappa}} = 10^{\Omega(l)}, \tag{14}$$

where

$$\Omega(l) = -\frac{(k_1+k_2)\,e(l)}{10} - \log\left(\frac{(d(l))^{\kappa}}{P(l)}\right).$$

The implementation of the controller (13) takes the actuator level constraints into account. Thus, the power control equation is defined as

$$d(l+1) = \left(\frac{P(l)}{10^{\Omega(l)}}\right)^{\frac{1}{\kappa}}, \tag{15}$$

and the corresponding distance control equation as

$$P(l+1) = 10^{\Omega(l)}(d(l+1))^{\kappa}. \tag{16}$$

VI. Stability Analysis

Let $V(e,l) : D \times [0,\infty) \to \mathbb{R}$ be a positive definite function defined as

$$V(e,l) = \frac{1}{2}e^2(l). \tag{17}$$

Taking the first difference of (17), substituting (8), we get

$$\begin{aligned}\Delta V(e,l) =& e(l)\Big\{10\log\left(\frac{10^{0.1\delta(l+1)}|X(l+1)|^2}{10^{0.1\delta(l)}|X(l)|^2}\right)\\ &+ 10\log\left(\frac{\eta(l+1)}{\eta(l)}\right) + u(l) + \xi(l)\Big\}\\ &+ (\Delta e(l))^2\end{aligned}$$

The term $(\Delta e(l))^2$ is controlled by controlling the sampling time T_s, and $E\left[e^2(l)\right] < b$ [15], $\Delta e(l)$ and hence $(\Delta e(l))^2$ can be assumed to be bounded by a constant say c. Using (9)-(12), and substituting (13) yields. Therefore

$$\Delta V \leq -k_1\,|e(l)|^2 + (c_1+c_2+c_3+c_5)\,|e(l)| - k_2\,|e(l)| + c \tag{18}$$

By completing the squares of (18), we get the inequality

$$\Delta V \leq -k_1\,|e(l)|^2 + \frac{(c_1+c_2+c_3+c_5)}{4k_2} + c.$$

Provided the sufficient condition of $0 < k_1 \leq 1$ is satisfied, Lemma 13.1 of [16] can be invoked to conclude that

$$\begin{aligned}V(e,l) \leq (1-k_1)^l\,V(e(l_0),l_0) + \left(\frac{1-(1-k_1)^l}{k_1}\right)\\ \cdot\left[\frac{(c_1+c_2+c_3+c_5)}{4k_2} + c\right],\end{aligned} \tag{19}$$

Based on (19), an upper bound for the SINR error can be developed as

$$\begin{aligned}|e(l)|^2 \leq (1-k_1)^l\,|e(l_0)|^2 + \left(\frac{1-(1-k_1)^l}{k_1}\right)\\ \cdot\left[\frac{(c_1+c_2+c_3+c_5)}{4k_2} + c\right].\end{aligned} \tag{20}$$

The inequality in (20) implies $e(l) \in \mathcal{L}_\infty$, and thus it can be used to conclude that $u(l) \in \mathcal{L}_\infty$ from (13), and hence $P(l+1), d(l+1) \in \mathcal{L}_\infty$ from (15) and (16) respectively. The ultimate bound in (20) asymptotically converges as

$$\lim_{l\to\infty}|e(l)|^2 \leq \frac{(c_1+c_2+c_3+c_5)^2}{4k_1k_2} + \frac{c}{k_1}. \tag{21}$$

From (21), the ultimate bound can be decreased by increasing k_1 and k_2; however, the magnitudes of k_1 and k_2 are restricted by the constraint that $0 < P_i(l) \leq P_{\max}$.

VII. Algorithm Design and Implementation

Our topology control algorithm combines information from the communications stack and the mobility of the platform. As we described in the previous sections, the control algorithms for mobility and power management have SINR as their objective function and independently adjust their control metrics (distance and power) to stabilize the system around a desired SINR. By tuning the control variables (k_1 and k_2), the response of the power control can be balanced with the mobility response.

While effective as a control strategy, the proposed design tends to keep the system operating at maximum power. Upon an immediate power adjustment, if the system reaches a point of desired SINR, there is no need for node mobility. Hence, we have modified equation (16) to maintain SINR as an objective function for a fixed power level to provide a more conservative response to sudden changes in distance. This modification enables the mobility controller to adjust the position of the follower to reach the desired SINR at a desired transmit power. The target power level P_{target} is set based on the context of the mission.

To illustrate our approach, we have used 50% of the maximum power as our desired power level. A higher threshold for the target power would progressively reduce the capacity of the controller to respond to sudden decreases in SINR, and a lower threshold would progressively increase such capacity, but it would require the follower to maintain close distance from the leader. While arbitrary at this point, the 50% level for target power offers a reasonable compromise between the two extremes and serves to illustrate the properties of the proposed mixed control strategy.

Consider a desired power level of P_{target}=.5P_{max}, we define the mobility control update as

$$d(l+1) = \left(\frac{P_{target}}{10^{\Omega(l)}}\right)^{\frac{1}{\kappa}}, \tag{22}$$

and the corresponding power control update as

$$P(l+1) = 10^{\Omega(l)}(d(l+1))^{\kappa}, \tag{23}$$

where

$$\Omega(l) = -\frac{(k_1+k_2)\,e(l)}{10} - \log\left(\frac{(d(l))^{\kappa}}{P(l)}\right).$$

Our approach enables a mixed control strategy for SINR management that combines a short-term power adaptation followed by a slower change in position, taking advantage of the differences in time-scale for the response of each component.

VIII. Experimental Evaluation

We created two simulation scenarios in NS-3 to evaluate our mixed control strategy. Each scenario consists of two airplanes, one being the leader and the other being the follower. The leader is actively tracking a high speed target in the ground and, while performing this task, it sends a stream of images to the follower, which we simulated as a fixed rate broadcast of constant size data packets.

To simplify the experimentation and focus on the performance of the control, we have considered SINR as the metric that represents the QoS requirements for the flow. In order to maintain the required QoS (i.e. fixed SINR), the follower can move closer or away from the leader. The follower can also increase or decrease its transmit power, which give the follower two control variables for link management.

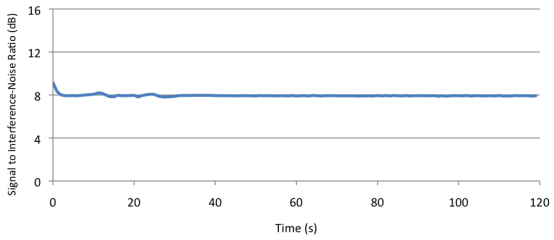

(a) SINR of the leader

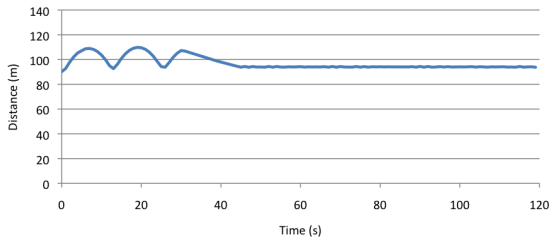

(b) Distance between follower and leader

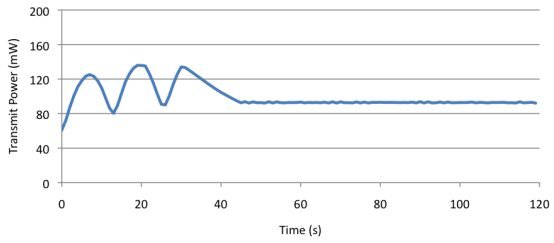

(c) Transmit power of the follower

Fig. 3. Mixed mobility and power control for SINR maintenance

In contrast with the example shown in Fig. 2, while there is an increase in distance between the platforms as the leader accelerates, the power control, as seen in 3(c), quickly compensates for the decrease in SINR, enabling the mobility control to slowly adjust the distance to the leader. As the follower approaches the leader, the power is progressively reduced to the target level (P_{target}). Sudden changes in the leader's trajectory will trigger power adjustments to compensate for the high frequency variations of SINR, while the longer term adaptation takes place.

In the previous example, the variations in SINR were solely caused by changes in relative position (distance) between two nodes. However, the controller can be easily extended to support multiple links. Let us consider a scenario where a follower UAV monitors the links to two leading UAVs (Fig. 4) and attempts to maintain a minimum SINR level with both. Each leader moves independently in a target tracking mission, while at the same time receives a control stream from the follower, which is operating as a relay for the two leading UAVs.

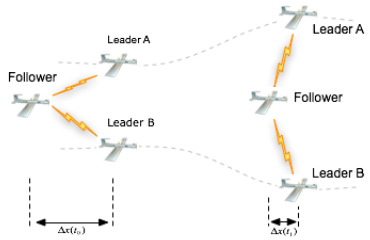

Fig. 4. Dual leading-node scenario

Monitoring each link independently, the follower maintains the SINR requirements to both leader platforms by controlling the transmit power settings and the distance towards both leaders. To the extend possible, the follower attempts to stay equidistant to both leaders while adjusting power as needed to compensate for high frequency variations.

The follower adjusts its position to maintain a target power (P_{target}) level of 50%. However, such condition can only be satisfied while the leaders remain within range. In the current version of our controllers, there is no prioritization among leaders, so it is possible that the follower will loose contact with both leaders if they move far enough away from each other. We can resolve this problem with a prioritization between leaders, in which case the follower chooses to abandon one of the leaders when is no longer capable to maintain connectivity with both.

As shown in Fig. 5, the mixed power control maintains the required SINR for each of the followers (Fig. 5(a)). The distance corrections (Fig. 5(b)) are the same for both leaders which indicates that the follower succeeded in making the target mobility corrections, while compensating for the fast changes in SINR through power control (Fig. 5(c)).

Since the follower has a single transmitter, thus a common power setting to both leader nodes, it compensates for differences in mobility or environmental effects through power adjustments. If leader A (Fig. 4) reported a lower SINR than leader B, possibly due to interference or shadowing, the follower would immediately adjust its transmit power and slowly reduce its distance to leader A in relation to leader B.

IX. Conclusion and Future Work

Topology management in tactical networks can be achieved through multiple control mechanisms at different levels in the

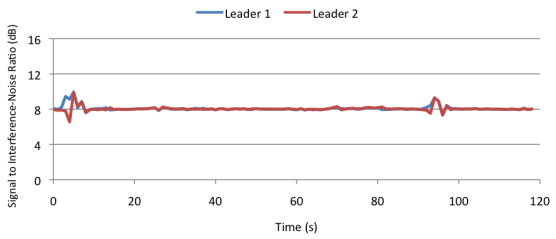

(a) SINR of the leaders

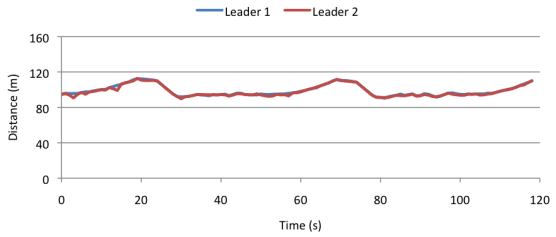

(b) Distance between follower and leaders

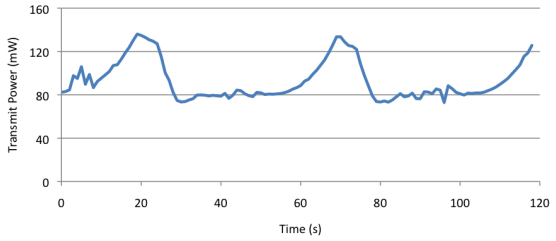

(c) Transmit power of the follower

Fig. 5. Mixed mobility and power control for multiple dual-link scenario

communications stack. In this paper we have introduced a mixed topology control algorithm that combines two control inputs (transmit power and node mobility) operating at different time scales. The concept is generally extensible to other control strategies and suggests that, if properly coordinated, mixed control strategies can accommodate both the transient and the steady state requirements of the system.

We tested our proof-of-concept implementation against simple simulated environments, showing encouraging results. While our studies are still preliminary at this point, we are confident that mixed control strategies can play an important role on protocols for topology management and control.

Our future work includes the implementation of the proposed strategy as a control module for XLayer [17], as well as the evaluation of the control algorithms under emulated and realistic timing requirements using MLAB [18], a hybrid emulation testbed developed in collaboration with the U.S. Air Force Research Laboratory that enables the use of theoretical and data-driven link emulation models for airborne networks.

Acknowledgment

This material is based on research sponsored by the Air Force Research Laboratory under agreement number FA8750-10-2-0145. The U.S. Government is authorized to reproduce and distribute reprints for Governmental purposes notwithstanding any copyright notation thereon.

References

[1] H. Takagi and L. Keinrock, "Optimal transmission ranges for randomly distributed packet radio terminals," *IEEE Trans. Communications*, 1984.

[2] L. Li, J. Y. Halpern, P. Bahl, Y.-M. Wang, and R. Wattenhofer, "Analysis of a cone-based distributed topology control algorithm for wireless multi-hop networks," in *PODC '01: Proceedings of the twentieth annual ACM symposium on Principles of distributed computing*. New York, NY, USA: ACM, 2001, pp. 264–273.

[3] M. Cardei, J. Wu, and S. Yang, "Topology control in ad hoc wireless networks using cooperative communication," *IEEE Transactions on Mobile Computing*, vol. 5, no. 6, pp. 711–724, 2006.

[4] T. Moscibroda and R. Wattenhofer, "Minimizing interference in ad hoc and sensor networks," in *DIALM-POMC '05: Proceedings of the 2005 joint workshop on Foundations of mobile computing*. New York, NY, USA: ACM, 2005, pp. 24–33.

[5] M. Burkhart, P. von Rickenbach, R. Wattenhofer, and A. Zollinger, "Does topology control reduce interference?" in *MobiHoc '04: Proceedings of the 5th ACM international symposium on Mobile ad hoc networking and computing*. New York, NY, USA: ACM, 2004, pp. 9–19.

[6] H. Chuanhe, C. Yong, L. Yuan, S. Wenming, and Z. Hao, "An interference-aware and power efficient topology control algorithm for wireless multi-hop networks," in *PERCOM '08: Proceedings of the 2008 Sixth Annual IEEE International Conference on Pervasive Computing and Communications*. Washington, DC, USA: IEEE Computer Society, 2008, pp. 330–335.

[7] P. Siripongwutikorn and B. Thipakorn, "Mobility-aware topology control in mobile ad hoc networks," *Comput. Commun.*, vol. 31, no. 14, pp. 3521–3532, 2008.

[8] M. Arguedas, C. Perez, M. Carvalho, A. Granados, K. Hoback, and W. Kraus, "Investigating the use of topology adaptation for robust multi-path transport: A preliminary study," in *2009 8th IEEE International Symposium on Network Computing and Applications, NCA 2009, July 9, 2009 - July 11, 2009*. Institute for Human and Machine Cognition, 40 S. Alcaniz St., Pensacola, FL 32502, United States: IEEE Computer Society, 2009, pp. 118–121.

[9] H. Zhu, K. Lu, and M. Li, "Distributed topology control in multi-channel multi-radio mesh networks," in *IEEE International Conference on Communications, ICC 2008, May 19, 2008 - May 23, 2008*. ArgonST/San Diego Research Center, San Diego, CA 92121, United States: Institute of Electrical and Electronics Engineers Inc., 2008, pp. 2958–2962.

[10] P. Santi, "Topology control in wireless ad hoc and sensor networks," *ACM Comput. Surv.*, vol. 37, no. 2, pp. 164–194, 2005.

[11] Z. Gengzhong and L. Qiumei, "A survey on topology control in wireless sensor networks," in *ICFN '10: Proceedings of the 2010 Second International Conference on Future Networks*. Washington, DC, USA: IEEE Computer Society, 2010, pp. 376–380.

[12] T. Zhang, K. Yang, and H.-H. Chen, "Topology control for service-oriented wireless mesh networks," *Wireless Commun.*, vol. 16, no. 4, pp. 64–71, 2009.

[13] R. Canchi and Y. Akaiwa, "Performance of adaptive transmit power control in $\pi/4$ DQPSK mobile radio systems in flat Rayleigh fading channels," in *Proc. IEEE Vehicular Technology Conference*, vol. 2, 16-20 May 1999, pp. 1261–1265.

[14] T. Rappaport, *Wireless Communications, Principles and Practice*. Prentice Hall, 1999.

[15] S. Subramanian, J. M. Shea, and W. E. Dixon, "Power control of cellular communications with channel uncertainties," in *Proc. American Control Conference*, 2009, pp. 1569–1574.

[16] J. Spooner, M. Maggiore, R. Ordonez, and K. Passino, *Stable Adaptive Control and Estimation for Nonlinear Systems*. Wiley, 2002.

[17] M. Carvalho, A. Granados, W. Naqvi, A. Brothers, J. P. Hanna, and K. Turck, "A cross-layer communications substrate for tactical information management systems," in *Military Communications Conference (MILCOM)*. IEEE, Nov. 2008.

[18] M. Carvalho, A. Granados, R. Carff, M. Arguedas, C. Perez, and D. Edwards, "MLAB: A hybrid emulation testbed," Institute for Human and Machine Cognition, Tech. Rep., January 2010.